

Available online at www.sciencedirect.com**ScienceDirect****NUCLEAR PHYSICS B**

Nuclear Physics B 913 (2016) 64–78

www.elsevier.com/locate/nuclphysb

Diphoton decay for a 750 GeV scalar boson in a $U(1)_X$ model

R. Martinez, F. Ochoa, C.F. Sierra*

Departamento de Física, Universidad Nacional de Colombia, Ciudad Universitaria, K. 45 No. 26-85, Bogotá D.C., Colombia

Received 28 July 2016; received in revised form 8 September 2016; accepted 8 September 2016

Available online 14 September 2016

Editor: Tommy Ohlsson

Abstract

In the context of a nonuniversal and anomaly free $U(1)_X$ extension of the standard model, we examine the decay of a 750 GeV scalar singlet state, ξ_X , as a possible explanation of the observed diphoton excess announced by the ATLAS and CMS collaborations at CERN-LHC collider. The one-loop decay to photons is allowed through three heavy singlet quarks and one charged Higgs boson into the loop. We obtain, for different width approximations and for masses of the exotic singlet quarks in the region [900, 3000] GeV, a production cross section $\sigma(pp \rightarrow \xi_X \rightarrow \gamma\gamma)$ compatible with ATLAS and CMS collaborations data. We also include another scalar singlet, σ , as a dark matter candidate that may couple with the 750 GeV scalar at tree level with production cross sections in agreement with ATLAS and CMS.

© 2016 The Authors. Published by Elsevier B.V. This is an open access article under the CC BY license (<http://creativecommons.org/licenses/by/4.0/>). Funded by SCOAP³.

1. Introduction

Although the Standard Model (SM) [1] is the simplest model that successfully explains most of the phenomena and experimental observations in particle physics, there are still some unexplained and unanswered fundamental questions which many theorists associate with an underlying theory beyond the SM. The most recent experimental discrepancy is the 3σ excess in the

* Corresponding author.

E-mail addresses: remartinezm@unal.edu.co (R. Martinez), faochoap@unal.edu.co (F. Ochoa), cfsierraf@unal.edu.co (C.F. Sierra).

diphoton channel at 750 GeV announced by the ATLAS and CMS collaborations [2,3] which has been the subject of many interpretations in the literature from different extensions of the standard model (SM) [4–12]. Although this observation requires further analyses and more experimental data, it is interesting to explore the theoretical and phenomenological consequences to have a new resonance with this mass. In particular, a scalar candidate is supported by many theoretical models, as for example, heavier Higgs bosons from scalar extensions of the SM, as recently considered in [13], models with heavy axion candidates as shown in [14] and with pseudo-Nambu Goldstone bosons as in [15]. Authors in [16] and [17] have studied general cases for different possible models.

In particular, nonuniversal $U(1)'$ symmetry models have many well-established motivations. First, since family representations are nonuniversal, they may provide hints for solving the SM flavor puzzle [18]. Secondly, these models contain an extra Z' neutral gauge boson with many interesting phenomenological consequences at low and high energies [19]. In some models, an extended fermion spectrum is necessary in order to obtain an anomaly-free theory, providing a natural scenario for extra charged leptons and/or heavy quarks. Also, the new symmetry requires an extended scalar sector in order to *i.*) generate the breaking of this symmetry and *ii.*) obtain heavy masses for the new Z' gauge boson and the extra fermion content. Another consequence of an extended Higgs sector is that they may produce deviations of the Higgs self-coupling, which could provide an interesting test for the SM Higgs boson from future measurements at the LHC collider [20].

In this paper, we evaluate the process of a 750 GeV scalar particle decaying into two photons in the context of the nonuniversal $U(1)_X$ extension introduced in Refs. [21–23], which gives us a natural scenario with one-loop contributions from heavy quarks and charged Higgs bosons. In section 2 we present the particle content of the model as well as the Higgs potential and the Yukawa Lagrangian. In section 3, we analyze the diphoton decay by using three approximations for the decay width. First, we assume that the total decay of the scalar candidate come only from one loop decay contributions. Second, we take the total width as $\Gamma = 45$ GeV, reported by the ATLAS Collaboration. Finally, we consider the decay into a scalar dark matter candidate, σ .

2. Description of the model

We consider the abelian extension $G_{sm} \times U(1)_X$, where $G_{sm} = (SU(3)_c, SU(2)_L, U(1)_Y)$ is the ordinary SM gauge symmetries, while $U(1)_X$ is an extra symmetry that assigns a new charge X to the particle content, as shown in Tables 1 and 2. Some general properties of the model are:

- In order to cancel the chiral anomalies, we demand that the equations that describe them be canceled, as shown in [21]. These equations lead us to a set of non-trivial solutions for $U(1)_X$ that requires a structure of three families. First, the left-handed leptons ℓ_L^i are universal of family, with charge $X_\ell = -1/3$. Second, the left-handed quarks q_L^i have nonuniversal charges: family with $i = 1$ has $X_1 = 1/3$, while $X_{2,3} = 0$ for $i = 2, 3$. In addition, the cancellation of anomalies requires the existence of an extended fermion sector. A simple possibility in the quark sector is by introducing quasi-chiral singlets (T and J^n , where $n = 1, 2$), i.e. singlets that are chiral under $U(1)_X$ and vector-like under the SM.
- An extra neutral gauge boson, Z'_μ , is required to make the $U(1)_X$ transformation a local symmetry.
- Due to the nonuniversal structure of the quark doublets, two scalar doublets ϕ_1 and ϕ_2 identical under G_{sm} but with $U(1)_X$ charges $X_{\phi_1} = 2/3$ and $X_{\phi_2} = 1/3$, respectively, are required

Table 1
Ordinary SM particle content, with $i = 1, 2, 3$.

Spectrum	G_{sm}	$U(1)_X$
$q_L^i = \begin{pmatrix} U^i \\ D^i \end{pmatrix}_L$	(3, 2, 1/3)	1/3 for $i = 1$ 0 for $i = 2, 3$
U_R^i	(3, 1, 4/3)	2/3
D_R^i	(3, 1, -2/3)	-1/3
$\ell_L^i = \begin{pmatrix} v^i \\ e^i \end{pmatrix}_L$	(1, 2, -1)	-1/3
e_R^i	(1, 1, -2)	-1
$\phi_1 = \begin{pmatrix} \phi_1^+ \\ \frac{v_1 + \xi_1 + i\xi_1}{\sqrt{2}} \end{pmatrix}$	(1, 2, 1)	2/3

Table 2
Extra non-SM particle content, with $n = 1, 2$.

Spectrum	G_{sm}	$U(1)_X$
T_L	(3, 1, 4/3)	1/3
T_R	(3, 1, 4/3)	2/3
J_L^n	(3, 1, -2/3)	0
J_R^n	(3, 1, -2/3)	-1/3
$\phi_2 = \begin{pmatrix} \phi_2^+ \\ \frac{1}{\sqrt{2}}(v_2 + \xi_2 + i\xi_2) \end{pmatrix}$	(1, 2, 1)	1/3
$\chi = \frac{1}{\sqrt{2}}(v_\chi + \xi_\chi + i\xi_\chi)$	(1, 1, 0)	-1/3
σ	(1, 1, 0)	-1/3
Z'_μ	(1, 1, 0)	0
$(v_R^i)^c$	(1, 1, 0)	-1/3
N_R^i	(1, 1, 0)	0

in order to obtain massive fermions after the spontaneous symmetry breaking, where the electroweak vacuum expectation value (VEV) is $v = \sqrt{v_1^2 + v_2^2}$.

- An extra scalar singlet χ , with $U(1)_X$ charge $X = -1/3$ and VEV v_χ is required to produce the symmetry breaking of the $U(1)_X$ symmetry. We assume that it happens at a large scale $v_\chi > v$. The real component ξ_χ remains in the particle spectrum after the symmetry breaking, and is our candidate to explain the 750 GeV signal. The imaginary component ζ_χ is the would-be Goldstone boson that provides mass to the extra neutral gauge boson Z' .
- Another scalar singlet, σ , is introduced, which is a scalar dark matter (DM) candidate. In order to reproduce the observed DM relic density, this particle must accomplish the following minima conditions [22,23]:
 - Since σ acquires a nontrivial charge $U(1)_X$, it must be complex in order to be a massive candidate.
 - To avoid odd powers terms in the scalar Lagrangian, which leads to unstable DM, we impose the global continuous symmetry

$$\sigma \rightarrow e^{i\theta} \sigma. \quad (1)$$

- (iii) In spite of the above symmetry, the model still can generate odd power terms via spontaneous symmetry breaking. To avoid this, σ must not generate VEV during the lifetime of our Universe.
- Extra discrete symmetries can be assumed in this model for scalar and quarks fields in order to obtain hierarchical mass structures, as shown in [21]. However, these types of symmetries do not affect the Yukawa couplings that participates in the diphoton signal. Thus, additional global symmetries will be irrelevant in our calculations.
- It is desirable to obtain a realistic model compatible with the oscillation of neutrinos. For this purpose, the model introduces new neutrinos, $(\nu_R^i)^c$ and N_R^i with $i = 1, 2, 3$ which may generate seesaw neutrino masses. However, this sector will be irrelevant in the present analysis.

2.1. Higgs potential

As shown in [22], the most general, renormalizable and $G_{sm} \times U(1)_X$ invariant potential with the symmetry $\sigma \rightarrow e^{i\theta}\sigma$ is

$$\begin{aligned}
V = & \mu_1^2 |\phi_1|^2 + \mu_2^2 |\phi_2|^2 + \mu_3^2 |\chi|^2 + \mu_4^2 |\sigma|^2 \\
& + f_2 \left(\phi_2^\dagger \phi_1 \chi + h.c. \right) \\
& + \lambda_1 |\phi_1|^4 + \lambda_2 |\phi_2|^4 + \lambda_3 |\chi|^4 + \lambda_4 |\sigma|^4 \\
& + |\phi_1|^2 \left[\lambda_6 |\chi|^2 + \lambda'_6 |\sigma|^2 \right] \\
& + |\phi_2|^2 \left[\lambda_7 |\chi|^2 + \lambda'_7 |\sigma|^2 \right] \\
& + \lambda_5 |\phi_1|^2 |\phi_2|^2 + \lambda'_5 \left| \phi_1^\dagger \phi_2 \right|^2 + \lambda_8 |\chi|^2 |\sigma|^2.
\end{aligned} \tag{2}$$

When we apply the minimum conditions $\partial \langle V \rangle / \partial v_i = 0$ for each scalar VEV $v_i = v_{1,2,\chi}$, following [22] we obtain at dominant order

$$\mu_3^2 \approx -\lambda_3 v_\chi^2, \tag{3}$$

which will allow us to obtain the mass of the real component of the scalar χ . With the above conditions, we get with an effective 2HDM type II, obtaining the squared mass matrices, for neutral real, neutral imaginary and charged scalar components. After diagonalization, we obtain three scalar mass eigenstates (h, H, H_ξ) from the real mass matrix, one pseudoscalar boson A from the imaginary matrix and one charged scalar H^\pm from the charged matrix. As shown in equation (4), the scalar Higgs boson H_ξ is identified with the real component ξ_χ , which is our 750 GeV candidate. There are also would-be Goldstone bosons that are absorbed as longitudinal components of the charged weak bosons W^\pm , and the two neutral gauge bosons Z and Z' . In the end, we obtain the following mass eigenvectors:

$$\begin{aligned}
\begin{pmatrix} G^\pm \\ H^\pm \end{pmatrix} &= R_\beta \begin{pmatrix} \phi_1^\pm \\ \phi_2^\pm \end{pmatrix}, \quad \begin{pmatrix} G \\ A \end{pmatrix} = R_\beta \begin{pmatrix} \xi_1 \\ \xi_2 \end{pmatrix}, \\
\begin{pmatrix} h \\ H \end{pmatrix} &= R_\alpha \begin{pmatrix} \xi_1 \\ \xi_2 \end{pmatrix}, \quad H_\chi \approx \xi_\chi, \quad G_\chi \approx \xi_\chi
\end{aligned} \tag{4}$$

where h is identified with the observed 125 GeV Higgs boson. The rotation matrices are defined according to

$$R_{\beta,\alpha} = \begin{pmatrix} C_{\beta,\alpha} & S_{\beta,\alpha} \\ -S_{\beta,\alpha} & C_{\beta,\alpha} \end{pmatrix}. \quad (5)$$

The rotation angles are β , defined as $\tan \beta = T_\beta = \frac{v_2}{v_1}$, and α obtained from the elements of the real mass matrix [22]

$$\tan 2\alpha \approx \tan 2\beta \left[1 + 2\sqrt{2}S_\beta C_\beta \left(\frac{\lambda_2 T_\beta^2 - \lambda_1}{T_\beta^2 - 1} \right) \left(\frac{v^2}{f_2 v_\chi} \right) \right]^{-1}, \quad (6)$$

where we have taken the dominant contribution assuming that $v^2 \ll |f_2 v_\chi|$. In Eq. (6), we can use the approximation

$$\tan 2\alpha \approx \tan 2\beta \quad (7)$$

as dominant contribution. After diagonalization of the real mass matrix, the mass of ξ_χ at dominant order is [21,22]

$$m_{\xi_\chi}^2 \approx 2\lambda_3 v_\chi^2. \quad (8)$$

On the other hand, we obtain all the couplings of the scalar χ with the above mass eigenstates. The sector of the potential associated to χ is:

$$V_\chi = \mu_3^2 |\chi|^2 + \lambda_3 |\chi|^4 + \lambda_6 |\chi|^2 |\phi_1|^2 + \lambda_7 |\chi|^2 |\phi_2|^2 + \lambda_8 |\chi|^2 |\sigma|^2. \quad (9)$$

After rotation to mass eigenvectors according to (4), we obtain all the interactions of χ with the scalar matter. In particular, for the real component ξ_χ of χ , we obtain:

$$V_{\xi_\chi} = \frac{1}{2} m_{\xi_\chi}^2 \xi_\chi^2 + v_\chi \xi_\chi \left\{ \left(\lambda_6 S_\beta^2 + \lambda_7 C_\beta^2 \right) |H^+|^2 + \lambda_8 \xi_\chi^2 |\sigma|^2 + \frac{1}{2} \left(\lambda_6 S_\alpha^2 + \lambda_7 C_\alpha^2 \right) H^2 + \frac{1}{2} \left(\lambda_6 C_\alpha^2 + \lambda_7 S_\alpha^2 \right) h^2 + \frac{1}{2} \left(\lambda_6 S_\beta^2 + \lambda_7 C_\beta^2 \right) A^2 \right\} \quad (10)$$

2.2. Yukawa Lagrangian

The most general, renormalizable, and $G_{sm} \times U(1)_X$ invariant Yukawa Lagrangian for quarks and with the global symmetry from Eq. (1) is:

$$\begin{aligned} -\mathcal{L}_Q = & \overline{q_L^1} \left(\tilde{\phi}_2 h_2^U \right)_{1j} U_R^j + \overline{q_L^a} \left(\tilde{\phi}_1 h_1^U \right)_{aj} U_R^j \\ & + \overline{q_L^1} \left(\phi_1 h_1^D \right)_{1j} D_R^j + \overline{q_L^a} \left(\phi_2 h_2^D \right)_{aj} D_R^j \\ & + \overline{q_L^1} \left(\phi_1 h_1^J \right)_{1m} J_R^m + \overline{q_L^a} \left(\phi_2 h_2^J \right)_{am} J_R^m \\ & + \overline{q_L^1} \left(\tilde{\phi}_2 h_2^T \right)_1 T_R + \overline{q_L^a} \left(\tilde{\phi}_1 h_1^T \right)_a T_R \\ & + \overline{T_L} \left(\chi^* h_\chi^U \right)_j U_R^j + \overline{T_L} \left(\chi^* h_T \right) T_R \\ & + \overline{J_L^n} \left(\chi h_\chi^D \right)_{nj} D_R^j + \overline{J_L^m} \left(\chi h_J \right)_{nm} J_R^m + h.c., \end{aligned} \quad (11)$$

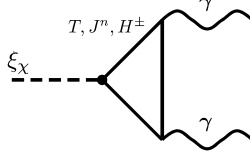


Fig. 1. Diphoton scalar decay mediated by quarks T , J^n and charged Higgs bosons H^\pm .

where $\tilde{\phi}_{1,2} = i\sigma_2\phi_{1,2}^*$ are conjugate scalar doublets, and $a = 2, 3$. We can see in Eq. (11) that due to the non-universality of the $U(1)_X$ symmetry, not all couplings between quarks and scalars are allowed by the gauge symmetry.

3. Diphoton decay

We take the real component ξ_χ of the field χ as our 750 GeV signal candidate, corresponding to the residual physical particle after the $U(1)_X$ symmetry breaking, while the imaginary component ζ_χ corresponds to the would-be Goldstone boson that becomes the longitudinal component of the Z' gauge boson. From the second term in expression (10), we can see that H^\pm couples to ξ_χ , contributing to the diphoton decay at one loop level. On the other hand, from the Yukawa Lagrangian in Eq. (11) we are interested in the coupling of the scalar singlet χ , which exhibits couplings with the heavy sector of the model and mixing terms with the ordinary SM quarks. The diphoton ξ_χ decay mediated by the T , J^n quarks and the charged Higgs boson H^\pm is as shown in Fig. 1.

3.1. Decay width

The masses of the extra neutral, pseudoscalar and charged Higgs bosons H , A and H^\pm , respectively, are nearly degenerate at the TeV scale, as shown in [21,22]. Then, the decay of ξ_χ into these Higgs bosons is kinematically forbidden. The decay into the observed Higgs boson $\xi_\chi \rightarrow hh$ is strongly constrained by ATLAS and CMS at 95%CL [16]. In this way, we obtain the following total decay width for ξ_χ :

$$\Gamma = \Gamma_{\gamma\gamma} + \Gamma_{gg} + \Gamma_{Z\gamma} + \Gamma_{ZZ} + \Gamma_{WW} + \Gamma_{\sigma^*\sigma} \quad (12)$$

We assume the following three scenarios for the total decay width of our 750 GeV candidate:

- First, we use one loop contributions, $\Gamma = \Gamma_{\gamma\gamma} + \Gamma_{gg} + \Gamma_{Z\gamma} + \Gamma_{ZZ} + \Gamma_{WW}$.
- Second, we use the experimentally reported width from the ATLAS Collaboration $\Gamma = 45$ GeV.
- Finally, we consider that the width is dominated by decays into the scalar dark matter particle σ , $\Gamma \simeq \Gamma(\xi_\chi \rightarrow \sigma^*\sigma)$.

For the last scenario, after replacing v_χ in terms of m_{ξ_χ} from Eq. (8), the total decay width is:

$$\Gamma \simeq \frac{\lambda_8 m_{\xi_\chi}}{32\pi} \sqrt{1 - \frac{4m_\sigma^2}{m_{\xi_\chi}^2}}. \quad (13)$$

For the decay of the ξ_χ particle into one loop contributions, we consider general interactions of the form

$$g_{\gamma H^+H^-} = \lambda (p_1 - p_2)^\mu, \quad g_{ZH^+H^-} = \lambda' (p_1 - p_2)^\mu, \quad (14)$$

$$g_{WH^+H^-} = \eta (p_1 - p_2)^\mu, \quad g_{WHH^\pm} = \eta' (p_1 - p_2)^\mu. \quad (15)$$

We also write the widths in terms of the Yukawa couplings of the top-like quark h_T and bottom-like quarks h_{J^1} , h_{J^2} , and the trilinear effective coupling with charged Higgs bosons defined as

$$h_{H^\pm} \equiv \left(\lambda_6 S_\beta^2 + \lambda_7 C_\beta^2 \right), \quad (16)$$

obtaining [24,25]:

$$\begin{aligned} \Gamma_{\gamma\gamma} &= \frac{\alpha^2 m_{\xi_X}}{32\pi^3} \left| \sum_i h_i N_i Q_i^2 F_i \right|^2, \\ \Gamma_{gg} &= \frac{\alpha_s^2 m_{\xi_X}}{16\pi^3} \left| \sum_{i \neq H^\pm} h_i F_i \right|^2, \\ \Gamma_{Z\gamma} &= \frac{\alpha^2 m_{\xi_X}}{16\pi^3} \left(1 - \frac{m_Z^2}{m_{\xi_X}^2} \right)^3 \left| \frac{2}{3} \sum_i h_i N_{ci} Q_i^2 + \frac{\lambda \lambda'}{24\pi\alpha} \right|^2, \\ \Gamma_{WW} &= \frac{\alpha^2 m_{\xi_X}}{4\pi^3} \mathcal{P} \left(\frac{m_W^2}{m_{\xi_X}^2} \right) \left| \frac{2}{3} \sum_i h_i N_{ci} Q_i^2 + \frac{\eta \eta'}{24\pi\alpha} \right|^2, \end{aligned} \quad (17)$$

$$\Gamma_{ZZ} = \frac{\alpha^2 m_{\xi_X}}{8\pi^3} \mathcal{P} \left(\frac{m_Z^2}{m_{\xi_X}^2} \right) \left| \frac{2}{3} \sum_i h_i N_{ci} Q_i^2 + \frac{\lambda^2}{24\pi\alpha} \right|^2 \quad (18)$$

where $\mathcal{P}(x) = \sqrt{1-4x} (1-4x+6x^2)$ is a factor correcting the massive final states in the decay width and

$$F_i = \begin{cases} -\sqrt{\tau_i} [1 + (1 - \tau_i) f(\tau_i)], & i = 1/2, \\ \sqrt{\tau_i} [1 - \tau_i f(\tau_i)] & i = 0, \end{cases}$$

with $h_i = h_T$, h_J , h_{H^\pm} and $\tau_i = 4m_i^2/m_{\xi_X}^2$ for $\tau_i > 1$, which requires that $m_i > 375$ GeV for a scalar particle of $m_{\xi_X} = 750$ GeV. The loop factor is:

$$f(\tau_i) = \left[\arcsin \left(\frac{1}{\sqrt{\tau_i}} \right) \right]^2. \quad (19)$$

We emphasize that although the $\xi_X hh$ coupling is strongly constrained by ATLAS and CMS data, it does not imply necessarily a suppression of the $\xi_X H^+H^-$ coupling. For example, if we set:

$$\lambda_6 S_\alpha^2 + \lambda_7 C_\alpha^2 \approx 0, \quad (20)$$

$$\lambda_6 S_\beta^2 + \lambda_7 C_\beta^2 = \lambda, \quad (21)$$

with λ the trilinear effective coupling defined in (16), we obtain:

$$\lambda_6 = \frac{-\lambda S_\beta^2}{C_\beta^2 - S_\alpha^2}, \quad \lambda_7 = \frac{\lambda C_\beta^2}{C_\beta^2 - S_\alpha^2}, \quad (22)$$

where we have used the approximation of Eq. (7), $\alpha \approx \beta$. In this way, ξ_X decouple from hh but not from H^+H^- .

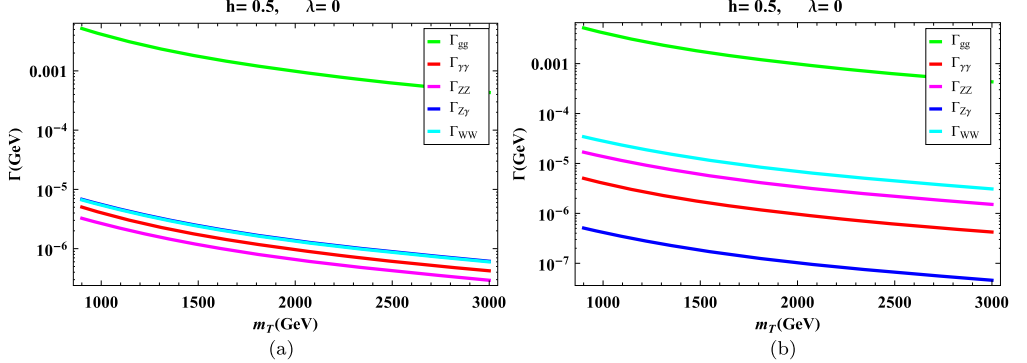


Fig. 2. Different decay channels for the 750 GeV candidate at one loop level.

3.2. Production cross section

The total cross section $\sigma(pp \rightarrow \xi_\chi \rightarrow \gamma\gamma)$ for a spin zero ξ_χ scalar is given by

$$\sigma(pp \rightarrow \xi_\chi \rightarrow \gamma\gamma) = \frac{C_{gg} \Gamma(\xi_\chi \rightarrow gg)}{s m_{\xi_\chi} \Gamma} \Gamma(\xi_\chi \rightarrow \gamma\gamma), \quad (23)$$

where

$$C_{gg} = \frac{\pi^2}{8} \int_{m_{\xi_\chi}/s}^1 \frac{dx}{x} g(x) g(m_{\xi_\chi}^2/sx) \quad (24)$$

is the dimensionless partonic integral. At the scale $\mu = m_{\xi_\chi} = 750$ GeV, and center-of-mass energy $\sqrt{s} = 13$ TeV, this integral gives $C_{gg} = 2137$ [26]. For the analysis, we take the combined results for the cross section from ATLAS and CMS, $\sigma(pp \rightarrow \xi_\chi \rightarrow \gamma\gamma) = (2-8)$ fb equally valid for $\sqrt{s} = 8$ TeV and $C_{gg} = 174$ [16]. In addition, we have assumed $\lambda = \lambda' = \eta = \eta'$, and $h = h_T = h_{J1} = h_{J2}$ for simplicity, i.e., $m_T = m_{J1} = m_{J2}$. We have taken $m_{H^\pm} = 400$ GeV which is the lowest bound reported from charged Higgs boson searches by ATLAS and CMS for a 2HDM type II [28]. Also, the lower bound of 900 GeV for m_T corresponds to the reported value in recent searches on top- and bottom-like heavy quarks from ATLAS and CMS Collaborations [27] and the upper bound of 3 TeV corresponds to the asymptotic value obtained from the fermionic form factor $F_{1/2}$.

For the case $\Gamma = \Gamma_{\gamma\gamma} + \Gamma_{gg} + \Gamma_{Z\gamma} + \Gamma_{ZZ} + \Gamma_{WW}$, we show in Fig. 2 the different contributions in Eq. (18) for the decay width of ξ . From Fig. 2 (a), the case $\lambda = 0$ and $h = 0.5$ corresponds to pure fermionic contributions into the loops. We can see that the contributions (ignoring the dominant Γ_{gg}) $\Gamma_{\gamma\gamma}$, Γ_{ZZ} , $\Gamma_{Z\gamma}$, Γ_{WW} have branching ratios of order 23%, 15%, 32%, 31% respectively. On the other hand, the case $\lambda = 0.5$ and $h = 0.5$ in Fig. 2 (b), corresponds to both fermionic and bosonic contributions into the loop with $BR_{\gamma\gamma}$, BR_{ZZ} , $BR_{Z\gamma}$, BR_{WW} of order 9%, 30%, 1%, 60% respectively.

In this way, and taking into account current bounds on $\Gamma_{Z\gamma}/\Gamma_{\gamma\gamma}$, $\Gamma_{ZZ}/\Gamma_{\gamma\gamma}$ and $\Gamma_{WW}/\Gamma_{\gamma\gamma}$ [29], we display in Fig. 3 contour plots of the production cross-section $\sigma(pp \rightarrow \xi_\chi \rightarrow \gamma\gamma)$ in the $\Gamma_{Z\gamma}/\Gamma_{\gamma\gamma}$ - $\Gamma_{ZZ}/\Gamma_{\gamma\gamma}$ plane. For simplicity, we have set $\lambda_{eff} \equiv \lambda = h$ in such a way that the contour plots only depend on m_T and λ_{eff} . In general, for low values of m_T the ratio $\Gamma_{Z\gamma}/\Gamma_{\gamma\gamma}$ is of order $\Gamma_{Z\gamma}/\Gamma_{\gamma\gamma} \sim 1$, and for larger values of m_T we have $\Gamma_{Z\gamma}/\Gamma_{\gamma\gamma} < 1$. We also observe

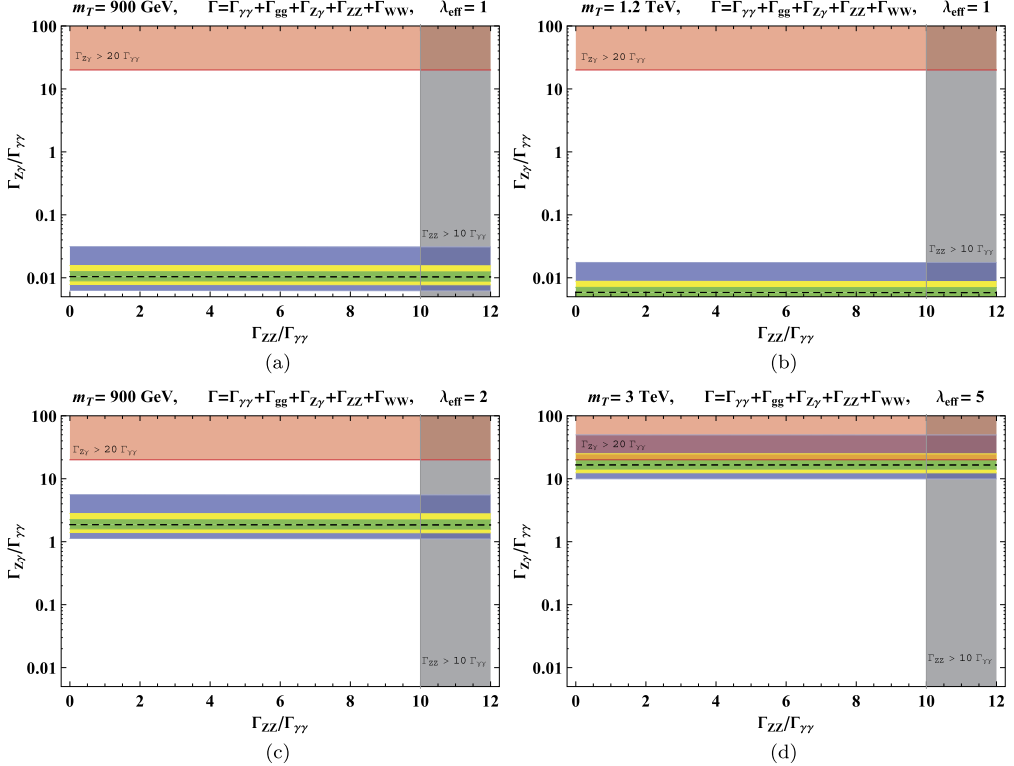


Fig. 3. Contour plots of the production cross-section $\sigma(pp \rightarrow \xi_\chi \rightarrow \gamma\gamma)$ in femtobarns. The dashed line corresponds to the central value at 6 fb, and the shaded bands correspond to regions at 68.3% (green), 95.5% (yellow) and 99.7% (light blue) C.L. exclusion limits from ATLAS and CMS combined data. The shaded red and gray regions are excluded. (For interpretation of the references to color in this figure legend, the reader is referred to the web version of this article.)

that the larger the ratio $\Gamma_{Z\gamma}/\Gamma_{\gamma\gamma}$, the stronger the coupling λ_{eff} . However, if $\lambda_{\text{eff}} > 5$ the model is completely excluded by the bound $\Gamma_{Z\gamma} < 20\Gamma_{\gamma\gamma}$ for all m_T .

On the other hand, in Fig. 4 (a) we use the width of $\Gamma = 45$ GeV reported by the ATLAS Collaboration for the scalar particle of 750 GeV, where we have used $m_{H^\pm} = 400$ GeV (the dependence on m_{H^\pm} is negligible in this case). In this case, the model is excluded for $m_T \geq 965$ GeV in the upper limit $h/4\pi = 1$ at 99% CL. For a narrower resonance we take $\Gamma = 1$ GeV in Fig. 4 (b), obtaining an allowed region for $900 \text{ GeV} \leq m_T < 2500 \text{ GeV}$ and $0.38 < h/4\pi \leq 1$. We observe that the larger the decay width, the smaller the allowed region.

Finally, we consider the tree level decay width into the dark matter candidate of the model, given by Eq. (13). We consider for the coupling constant, values in the range $0.15 \leq \lambda_8 \leq 3$ and for the decay width in the range $1.2 \text{ GeV} \leq \Gamma \leq 23 \text{ GeV}$. If $\lambda_8 \sim 0.15$, the width of the 750 GeV candidate is $\Gamma(\xi_\chi \rightarrow \sigma^*\sigma) \sim 1 \text{ GeV}$. Thus, this decay channel become in the dominant contribution, larger than the loop contributions. We also see that the dark matter decay width is sensitive to its mass m_σ only near to the kinematical region. In Fig. 5, we show the production cross section contours for $m_\sigma \approx m_h = 125$ GeV. In Figs. 5(a) and (b), we set $\lambda_8 = 0.15$ and a decay width of $\Gamma = 1.2 \text{ GeV}$ for $m_{H^\pm} = 400$ GeV and $m_{H^\pm} = 3.0 \text{ TeV}$ respectively. For this set of parameters in Figs. 5(a) and (b) the model is excluded for exotic quark masses greater

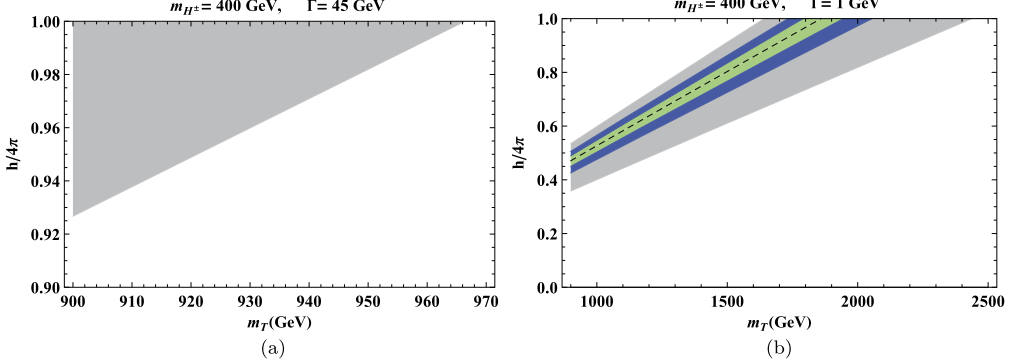


Fig. 4. Contours of the production cross-section $\sigma(pp \rightarrow \xi\chi \rightarrow \gamma\gamma)$ in femtobarns for (a) $\Gamma = 45$ GeV and (b) $\Gamma = 1$ GeV. The shaded gray regions correspond to 99% CL exclusion limits from ATLAS and CMS combined data, while the green and blue bands represent 68% CL and 95% CL ranges, respectively, around the best fit cross-section at 6 femtobarns. (For interpretation of the references to color in this figure legend, the reader is referred to the web version of this article.)

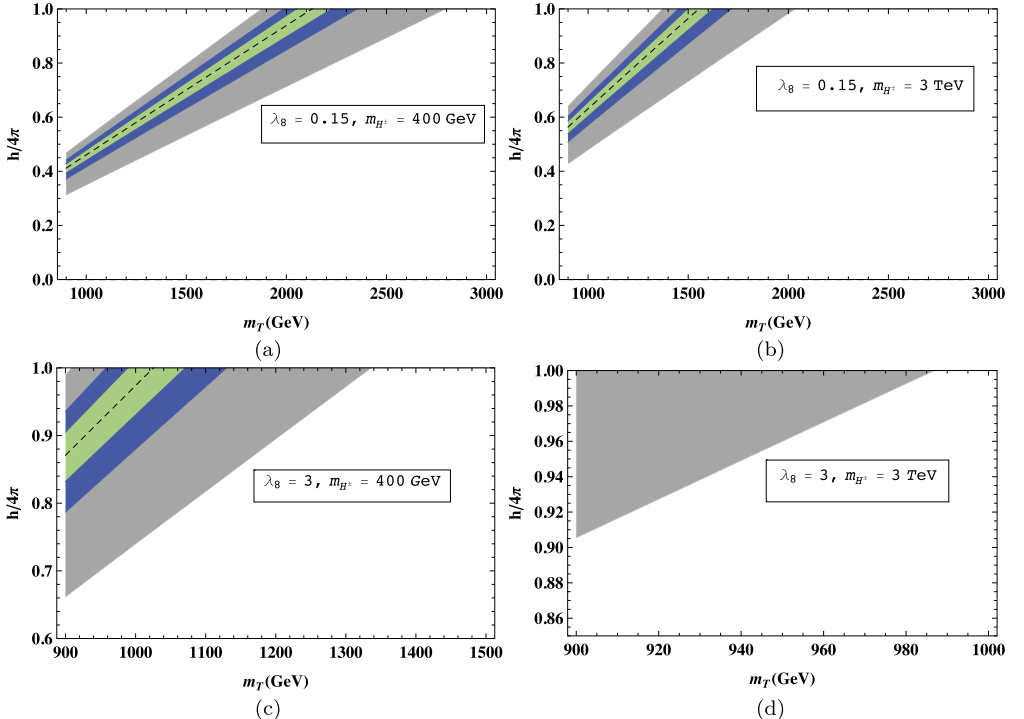


Fig. 5. Contour plots of the production cross-section $\sigma(pp \rightarrow \xi\chi \rightarrow \gamma\gamma)$ in femtobarns with $\Gamma \simeq \Gamma(\xi\chi \rightarrow \sigma^*\sigma)$. The shaded gray regions correspond to 99% CL exclusion limits from ATLAS and CMS combined data, while the green and blue bands represent 68% CL and 95% CL ranges, respectively, around the best fit cross-section at 6 femtobarns. (For interpretation of the references to color in this figure legend, the reader is referred to the web version of this article.)

than 2.7 TeV and 2.0 TeV respectively. In Figs. 5(c) and (d) we set $\lambda_8 = 3$ with a decay width of $\Gamma = 23$ GeV and the same values for m_{H^\pm} as before. In this case the model is excluded for $m_T > 1.3$ TeV in Fig. 5(c) and $m_T > 0.98$ TeV in Fig. 5(d).

4. Conclusions

Since the announcement of the ATLAS and CMS collaborations of a possible 750 GeV diphoton excess, many authors have attempted to explain the signal in the framework of several extensions of the SM that includes some type of resonance compatible with the reported data. In this work, we use a well-founded nonuniversal $U(1)_X$ extension that includes an extra particle sector, with a neutral scalar singlet being the candidate for the 750 GeV signal. Finding non-trivial solutions for the $U(1)_X$ charge that cancel the chiral anomalies, the model requires a structure of three fermion families, and an extension of the quark sector, being the most simple one top-like and two bottom-like quasi-chiral singlets. In addition, the model contains two Higgs doublets in order to provide masses to all fermions. In particular, after the symmetry breaking, one charged Higgs boson that couples with the scalar singlet is obtained. Thus, in a natural way, the model predicts a diphoton decay of the scalar singlet through one-loop corrections mediated by quark singlets and a charged Higgs boson. Finally, we include another scalar singlet with a $U(1)$ global symmetry as candidate for dark matter, and that also may couple with the 750 GeV scalar at tree level, contributing to the decay width. We found allowed regions in different scenarios compatible with a 750 GeV signal for masses of the top-like quark in the range $0.9 < m_T < 3$ TeV and charged Higgs bosons at 0.4 and 3 TeV.

Note added: While this manuscript was under review, the new 2016 LHC data for $(12.2 + 12.9) \text{ fb}^{-1}$ has confirmed no 750 GeV $\gamma\gamma$ excess [30].

Acknowledgements

This work was supported by El Patrimonio Autónomo Fondo Nacional de Financiamiento para la Ciencia, la Tecnología y la Innovación Francisco José de Caldas programme of COLCIENCIAS in Colombia.

References

- [1] S.L. Glashow, Nucl. Phys. 22 (1961) 579;
S. Weinberg, Phys. Rev. Lett. 19 (1967) 1264;
A. Salam, in: N. Svartholm (Ed.), Elementary Particle Theory: Relativistic Groups and Analyticity, Nobel Symposium No. 8, Almqvist and Wiksell, Stockholm, 1968, p. 367.
- [2] Talk by Jim Olsen, CMS Collaboration, CMS 13 TeV Results, CERN Jamboree, December 15, 2015. Plots are presented in: <http://cms-results.web.cern.ch/cms-results/public-results/preliminary-results/LHC-Jamboree-2015/index.html>.
- [3] Talk by Marumi Kado, ATLAS Collaboration, ATLAS 13 TeV Results, CERN Jamboree, December 15, 2015. Plots are presented in: <https://twiki.cern.ch/twiki/bin/view/>.
- [4] Y. Mambrini, G. Arcadi, A. Djouadi, arXiv:1512.04913;
M. Backovic, A. Mariotti, D. Redigolo, arXiv:1512.04917;
A. Angelescu, A. Djouadi, G. Moreau, arXiv:1512.04921;
Y. Nakai, R. Sato, K. Tobioka, arXiv:1512.04924;
S. Knapen, T. Melia, M. Papucci, K. Zurek, arXiv:1512.04928;
R. Franceschini, et al., arXiv:1512.04933;
S.D. McDermott, P. Meade, H. Ramani, arXiv:1512.05326;

- R. Benbrik, C.-H. Chen, T. Nomura, arXiv:1512.06028;
 M. Low, A. Tesi, L.-T. Wang, arXiv:1512.05328;
 B. Bellazzini, R. Franceschini, F. Sala, J. Serra, arXiv:1512.05330;
 R.S. Gupta, et al., arXiv:1512.05332;
 C. Peterson, R. Torre, arXiv:1512.05333;
 E. Molinaro, F. Sannino, N. Vignaroli, arXiv:1512.05334.
- [5] B. Dutta, et al., arXiv:1512.05439;
 Q.-H. Cao, et al., arXiv:1512.05542;
 S. Matsuzaki, K. Yamawaki, arXiv:1512.05564;
 A. Kobakhidze, et al., arXiv:1512.05585;
 P. Cox, A.D. Medina, T.S. Ray, A. Spray, arXiv:1512.05618;
 D. Beccirevic, E. Bertuzzo, O. Sumensari, R.Z. Funchal, arXiv:1512.05623;
 J.M. No, V. Sanz, J. Setford, arXiv:1512.05700;
 S.V. Demidov, D.S. Gorunov, arXiv:1512.05723;
 W. Chao, R. Huo, J. Yu, arXiv:1512.05738;
 S. Fichet, G.V. Gersdorff, C. Royon, arXiv:1512.05751;
 D. Curtin, C.B. Verhaaren, arXiv:1512.05753;
 L. Bian, N. Chen, D. Liu, J. Shu, arXiv:1512.05759;
 J. Chakrabortty, et al., arXiv:1512.05767;
 A. Ahmed, et al., arXiv:1512.05771;
 C. Csaki, J. Hubisz, J. Terning, arXiv:1512.05776;
 A. Falkowski, O. Sloane, T. Volaksy, arXiv:1512.05777;
 D. Aloni, et al., arXiv:1512.05778;
 Y. Bai, J. Berger, R. Lu, arXiv:1512.05779.
- [6] E. Gabrielli, et al., arXiv:1512.05961;
 J.S. Kim, J. Reuter, K. Rolbiecki, R.R. de Austri, arXiv:1512.06083;
 A. Alves, A.G. Dias, K. Sinha, arXiv:1512.06091;
 E. Megias, O. Pujolas, M. Quiros, arXiv:1512.06106;
 L.M. Carpenter, R. Colburn, J. Goodman, arXiv:1512.06107;
 J. Bermon, C. Smith, arXiv:1512.06113;
 W. Chao, arXiv:1512.06297;
 M.T. Arun, P. Saha, arXiv:1512.06335;
 C. Han, H.M. Lee, M. Park, V. Sanz, arXiv:1512.06376;
 S. Chang, arXiv:1512.06426;
 M. Luo, et al., arXiv:1512.06670.
- [7] I. Chakraborty, A. Kundu, arXiv:1512.06508;
 R. Ding, L. Huang, T. Li, B. Zhu, arXiv:1512.06560;
 H. Han, S. Wang, S. Zheng, arXiv:1512.06562;
 X.-F. Han, L. Wang, arXiv:1512.06587;
 J. Chang, K. Cheung, C. Lu, arXiv:1512.06671;
 D. Bardhan, et al., arXiv:1512.06674;
 T.-F. Feng, X.-Q. Li, H.-B. Zhang, S.-M. Zhao, arXiv:1512.06696;
 O. Antipin, M. Mojaza, F. Sannino, arXiv:1512.06708;
 F. Wang, L. Wu, J.M. Yang, M. Zhang, arXiv:1512.06715;
 J. Cao, et al., arXiv:1512.06728;
 F.P. Huang, C.S. Li, Z.L. Liu, Y. Wang, arXiv:1512.06732;
 W. Liao, H.-Q. Zheng, arXiv:1512.06741;
 J.J. Heckman, arXiv:1512.06773;
 M. Dhuria, G. Goswami, arXiv:1512.06782;
 X.-J. Bi, Q.-F. Xiang, P.-F. Yin, Z.-H. Yu, arXiv:1512.06787;
 J.S. Kim, K. Rolbiecki, R.R. de Austri, arXiv:1512.06797;
 L. Berthier, J.M. Cline, W. Shepherd, M. Trott, arXiv:1512.06799;
 W.S. Cho, et al., arXiv:1512.06824;
 J.M. Cline, Z. Liu, arXiv:1512.06827;
 M. Bauer, M. Neubert, arXiv:1512.06828;
 M. Chala, M. Duerr, F. Kahlhoefer, K.S. Hoberg, arXiv:1512.06833;

- D. Barducci, et al., arXiv:1512.06842.
- [8] S.M. Boucenna, S. Morisi, A. Vicente, arXiv:1512.06878;
 C.W. Murphy, arXiv:1512.06976;
 A.E.C. Hernandez, I. Nisandzic, arXiv:1512.07165;
 U.K. Dey, S. Mohanty, G. Tomar, arXiv:1512.07212;
 G.M. Pelaggi, A. Strumia, E. Vigiani, arXiv:1512.07225;
 J. de Blas, J. Santiago, R. Vega-Morales, arXiv:1512.07229;
 A. Belyaev, et al., arXiv:1512.07242;
 P.S.B. Dev, D. Teresi, arXiv:1512.07243;
 S. Moretti, K. Yagyu, arXiv:1512.07462;
 K.M. Patel, P. Sharma, arXiv:1512.7468;
 M. Badziak, arXiv:1512.07497;
 S. Chakraborty, A. Chakraborty, S. Raychaudhuri, arXiv:1512.07527;
 W. Altmannshofer, et al., arXiv:1512.07616;
 M. Cvetic, J. Halverson, P. Langacker, arXiv:1512.07622;
 J. Gu, Z. Liu, arXiv:1512.07624.
- [9] Q.-H. Cao, S.-L. Chen, P.-H. Gu, arXiv:1512.07541;
 P. Dev, R.N. Mohapatra, Y. Zhang, arXiv:1512.08507;
 B.C. Allanach, P. Dev, S.A. Renner, K. Sakurai, arXiv:1512.07645;
 H. Davoudiasl, C. Zhang, arXiv:1512.07672;
 N. Craig, P. Draper, C. Kilic, S. Thomas, arXiv:1512.07733;
 K. Das, S.K. Rai, arXiv:1512.07789;
 K. Cheung, et al., arXiv:1512.07853;
 J. Liu, X.-P. Wang, W. Xue, arXiv:1512.07885;
 J. Zhang, S. Zhou, arXiv:1512.07889;
 J.A. Casas, J.R. Espinosa, J.M. Moreno, arXiv:1512.07895;
 L.J. Hall, K. Harigaya, Y. Nomura, arXiv:1512.07904.
- [10] H. Han, S. Wang, S. Zheng, S. Zheng, arXiv:1512.07992;
 J.-C. Park, S.C. Park, arXiv:1512.08117;
 A. Salvio, A. Mazumdar, arXiv:1512.08184;
 D. Chway, R. Dermivsek, T.H. Jung, H.D. Kim, arXiv:1512.08221;
 G. Lo, et al., arXiv:1512.08255;
 M. Son, A. Urbano, arXiv:1512.08307;
 Y.-L. Tang, S.-H. Zhu, arXiv:1512.08323;
 H. An, C. Cheung, Y. Zhang, arXiv:1512.08378;
 J. Cao, F. Wang, Y. Zhang, arXiv:1512.08392;
 F. Wang, et al., arXiv:1512.08434;
 C. Cai, Z.-H. Yu, H. Zhang, arXiv:1512.08440;
 Q.-H. Cao, et al., arXiv:1512.08441;
 J.E. Kim, arXiv:1512.08467;
 J. Gao, H. Zhang, H.X. Zhu, arXiv:1512.08478;
 W. Chao, arXiv:1512.08484;
 X.-J. Bi, et al., arXiv:1512.08497;
 F. Goertz, J.F. Kamenik, A. Katz, M. Nardecchia, arXiv:1512.08500;
 L.A. Anchordoqui, I. Antoniadis, H. Goldberg, X. Huang, arXiv:1512.08502;
 N. Bizot, S. Davidson, M. Frigerio, J.-L. Kneur, arXiv:1512.08508;
 K. Kaneta, S. Kang, H.-S. Lee, arXiv:1512.09129;
 I. Low, J. Lykken, arXiv:1512.09089.
- [11] L.E. Ibanez, V.M. Lozano, arXiv:1512.08777;
 E. Ma, arXiv:1512.09159;
 L. Marzola, et al., arXiv:1512.09136;
 Y. Jiang, Y.-Y. Li, T. Liu, arXiv:1512.09127;
 A.E.C. Hernandez, arXiv:1512.09092;
 S. Kanemura, N. Machida, S. Odori, T. Shindou, arXiv:1512.09053;
 S. Kanemura, et al., arXiv:1512.09048;
 X.-J. Huang, W.-H. Zhang, Y.-F. Zhou, arXiv:1512.08992;

- Y. Hamada, T. Noumi, S. Sun, G. Shiu, arXiv:1512.08984;
 S.K. Kang, J. Song, arXiv:1512.08963;
 C.-W. Chiang, M. Ibe, T.T. Yanagida, arXiv:1512.08895;
 A. Dasgupta, M. Mitra, D. Borah, arXiv:1512.09202.
- [12] A.E. Faraggi, J. Rizos, arXiv:1601.03604;
 A. Djouadi, J. Ellis, R. Godbole, J. Quevillon, arXiv:1601.03696;
 J.H. Davis, M. Fairbairn, J. Heal, P. Tunney, arXiv:1601.03153;
 R. Ding, Z.-L. Han, Y. Liao, X.-D. Ma, arXiv:1601.02714;
 M. Fabbrichesi, A. Urbano, arXiv:1601.02447;
 J. Cao, et al., arXiv:1601.02570;
 P. Ko, T. Nomura, arXiv:1601.02490;
 S. Fichet, G. von Gersdorff, C. Royon, arXiv:1601.01712;
 I. Sahin, arXiv:1601.01676;
 D. Borah, S. Patra, S. Sahoo, arXiv:1601.01828;
 S. Bhattacharya, S. Patra, N. Sahoo, N. Sahu, arXiv:1601.01569;
 F. D'Eramo, J. de Vries, P. Panci, arXiv:1601.01571;
 H. Ito, T. Moroi, Y. Takaesu, arXiv:1601.01144;
 A.E.C. Hernandez, I.d.M. Varzielas, E. Schumacher, arXiv:1601.00661;
 T. Modak, S. Sadhukhan, R. Srivastava, arXiv:1601.00836;
 C. Csaki, J. Hubisz, S. Lombardo, J. Terning, arXiv:1601.00638;
 U. Danielsson, R. Enberg, G. Ingelman, T. Mandal, arXiv:1601.00624;
 D. Palle, arXiv:1601.00618;
 K. Ghorbani, H. Ghorbani, arXiv:1601.00602;
 X-F. Han, et al., arXiv:1601.00534;
 E. Palti, arXiv:1601.00285;
 P. Ko, Y. Omura, C. Yu, arXiv:1601.00586;
 T. Nomura, H. Okada, arXiv:1601.00386;
 H. Zhang, arXiv:1601.01355;
 S. Jung, J. Song, Y.W. Yoon, arXiv:1601.00006;
 I. Dorsner, S. Fajfer, N. Kosnik, arXiv:1601.03267;
 C. Hati, arXiv:1601.02457;
 D. Stolarski, R.V. Morales, arXiv:1601.02004;
 A. Berlin, arXiv:1601.01381;
 F.F. Deppisch, C. Hati, S. Patra, P. Pritimita, U. Sarkar, arXiv:1601.00952;
 B. Dutta, et al., arXiv:1601.00866;
 A. Karozas, S.F. King, G.K. Leontaris, A.K. Meadowcroft, arXiv:1601.00640;
 W. Chao, arXiv:1601.00633;
 W. Chao, arXiv:1601.04678;
 C.T. Potter, arXiv:1601.00240;
 A. Ghoshal, arXiv:1601.04291;
 T. Nomura, H. Okada, arXiv:1601.04516.
- [13] Dario Buttazzo, Admir Greljo, David Marzocca, arXiv:1512.04929.
- [14] A. Pilaftsis, arXiv:1512.04931.
- [15] Keisuke Harigaya, Yasunori Nomura, arXiv:1512.04850.
- [16] John Ellis, Sebastian A.R. Ellis, J. Quevillon, Veronica Sanz, Tevong You, arXiv:1512.05327.
- [17] Florian Staub, et al., arXiv:1602.05581.
- [18] P. Langacker, M. Plumacher, Phys. Rev. D 62 (2000) 013006;
 K. Leroux, D. London, Phys. Lett. B 526 (2002) 97;
 S. Baek, J.H. Jeon, C.S. Kim, Phys. Lett. B 641 (2006) 183.
- [19] For a review see A. Leike, Phys. Rep. 317 (1999) 143;
 J. Erler, P. Langacker, T.J. Li, Phys. Rev. D 66 (2002) 015002;
 S. Hesselbach, F. Franke, H. Fraas, Eur. Phys. J. C 23 (2002) 149.
- [20] Rick S. Gupta, Heidi Rzebak, James D. Wells, Phys. Rev. D 88 (2013) 055024, arXiv:1305.6397 [hep-ph];
 Aielet Efrati, Yosef Nir, arXiv:1401.0935 [hep-ph].
- [21] R. Martinez, J. Nisperuza, F. Ochoa, J.P. Rubio, Phys. Rev. D 89 (2014) 056008, arXiv:1303.2734.
- [22] R. Martinez, J. Nisperuza, F. Ochoa, J.P. Rubio, Phys. Rev. D 90 (2014) 095004, arXiv:1408.5153.

- [23] R. Martinez, J. Nisperuza, F. Ochoa, J.P. Rubio, C.F. Sierra, Phys. Rev. D 92 (2015) 035016, arXiv:1411.1641.
- [24] J.F. Gunion, H.E. Haber, G. Kane, S. Dawson, *The Higgs Hunter's Guide*, Addison-Wesley Publishing Company, 1990;
R. Martinez, M.A. Perez, J.J. Toscano, Phys. Rev. D 40 (1989) 1722;
R. Martinez, M.A. Perez, J.J. Toscano, Phys. Lett. B 234 (1990) 503;
R. Martinez, M.A. Perez, Nucl. Phys. B 347 (1990) 105–119.
- [25] Qing-Hong Cao, Yandong Liu, Ke-Pan Xie, Bin Yan, Dong-Ming Zhang, Phys. Rev. D 93 (2016) 075030.
- [26] M. Spira, A. Djouadi, D. Graudenz, P.M. Zerwas, Higgs boson production at the LHC, Nucl. Phys. B 453 (1995) 17, arXiv:hep-ph/9504378;
A.D. Martin, W.J. Stirling, R.S. Thorne, G. Watt, Parton distributions for the LHC, Eur. Phys. J. C 63 (2009) 189, arXiv:0901.0002.
- [27] CMS Collaboration, Phys. Rev. D 93 (2016) 012003;
ATLAS Collaboration, arXiv:1602.05606;
CMS Collaboration, arXiv:1507.07129.
- [28] ATLAS Collaboration, J. High Energy Phys. 03 (2016) 127;
CMS Collaboration, J. High Energy Phys. 12 (2015) 178;
CMS Collaboration, arXiv:1508.07774.
- [29] Roberto Franceschini, Gian F. Giudice, Jernej F. Kamenik, Matthew McCullough, Francesco Riva, Alessandro Strumia, Riccardo Torre, arXiv:1604.06446.
- [30] Talks at the 38th International Conference on High Energy Physics, by B. Lenzi (ATLAS collaboration) and by C. Rovelli (CMS collaboration).